Kotzé *Earth, Planets and Space* (2017) 69:84
DOI 10.1186/s40623-017-0670-y

Earth, Planets and Space

FULL PAPER



# Statistical evaluation of global geomagnetic field models over Southern Africa during 2015

P. B. Kotzé*

## Abstract

Global geomagnetic field models using spherical harmonic basis functions are important in space physics research, space weather and applications like navigation and mineral resources exploration. These models are based on various geomagnetic field data sets ranging from Earth surface magnetic observatory measurements to low-Earth orbit satellites equipped with highly sensitive and accurate magnetometers. Although these field models are derived by fitting harmonic functions to data distributed across the Earth, they are applied on regional scales within fixed boundaries in many instances and one can therefore question how well do these models perform on restricted areas. Three recently published global geomagnetic field models, IGRF-12, CHAOS-6 and POMME-10, have been statistically evaluated over Southern Africa using repeat station data as well as measurements from 4 INTERMAGNET observatories located at Hermanus and Hartebeesthoek in South Africa as well as Tsumeb and Keetmanshoop in Namibia for 2015. Apart from the observatory data, the field survey repeat station data do not form part of the data set on which these global field models are based and therefore can be regarded as an independent test of these field models over an area like Southern Africa which is well known for its rapid change of the geomagnetic field. Results obtained in this investigation for both main field and secular variation models clearly showed the importance of timely ground-based geomagnetic field observations in the derivation of accurate field models, particularly in regions characterised by rapid and unpredictable secular variation changes.

**Keywords:** Geomagnetism, Geomagnetic field models, Field surveys

## Introduction

The Earth's magnetic field, originating predominantly in the liquid outer core through a self-sustaining dynamo action, has been observed in a systematic way since the middle of the nineteenth century at various positions around the globe. Since the space age was established, satellites with high-precision magnetometers provided global coverage of the geomagnetic field, enabling the derivation of several geomagnetic field models to characterise various aspects of the Earth's magnetic field, e.g. MAGSAT (Langel and Estes 1985), Ørsted (Olsen 2002), CHAMP (Sabaka et al. 2004) and SWARM (Olsen et al. 2013). Recently three spherical harmonic-based global geomagnetic field models, IGRF-12 (Thébault et al. 2015), CHAOS-6 (Finlay et al. 2016) and POMME-10 (www.geomag.org/models/pomme10.html), using various combinations of observatory and satellite data, were published to describe the Earth's magnetic field and its time variation.

The International Geomagnetic Reference Field (IGRF) was introduced by the International Association of Geomagnetism and Aeronomy (IAGA) in 1968 in response to the demand for a standard spherical harmonic representation of the Earth's main field. The model is updated at 5-yearly intervals, the latest being the 12th generation, produced and released by IAGA Working Group V-MOD in December 2014 and therefore could not utilise any Southern African geomagnetic field data for 2015. This particular version consists of new models for epochs

*Correspondence: pkotze@sansa.org.za
South African National Space Agency (SANSA), Space Science, Hermanus, South Africa

2010 (DGRF-2010) and 2015 (IGRF-2015) as well as a predictive secular variation model for 2015–2020 (SV 2015–2020). These models were derived from weighted averages of candidate models submitted by several international institutions.

CHAOS-6, on the other hand, is the latest in the CHAOS series of global geomagnetic field models which aims to model the Earth's magnetic field at ground level. More than 2 years of SWARM data together with monthly means from 160 observatories available till March 2016 were used to update the CHAOS time-dependent model to provide information on the time-dependant behaviour of the core main field part of the geomagnetic field between 1999.0 and 2016.5. CHAOS-6 also benefits from vector data from Ørsted and CHAMP in addition to the 3 SWARM satellites. One difference with previous models is that vector data from CHAMP were only used when both star cameras provided attitude information. This is also the first member of the CHAOS series of field models to utilise spatial field differences as data from both CHAMP and SWARM satellites (Finlay et al. 2016). Southern African observatory data for 2015 were therefore used in the derivation of this particular model, but not the repeat station observations.

The POMME series of geomagnetic field models are mathematical models representing main geomagnetic field to degree and order 15 as well as the crustal field to degree and order 133 which distinguishes it from the other two models. In this investigation, only the main field module was utilised. The time variations of the internal field are parameterised by a piecewise linear representation of the spherical harmonic coefficients. POMME-10 was derived from CHAMP satellite vector magnetic measurements from July 2000 to including September 2010, Ørsted total field measurements from January 2010 to June 2014 as well as SWARM satellite vector magnetic measurements ranging from December 2013 to November 2015 (www.geomag.org/models/pomme10.html). POMME-10 therefore did not utilise any ground-based observatory or field survey data from Southern Africa measured during 2015.

Global geomagnetic field models like IGRF-12, CHAOS-6 and POMME-10 are important tools utilised by researchers and commercial users to obtain various characteristic parameters of the Earth's magnetic field as a function of time and geographic position (latitude, longitude and altitude). A substantial proportion of these applications are for restricted areas or single positions. The question therefore arises as to how well these global field models represent the geomagnetic field on a regional basis, particularly a region such as Southern Africa which is well known for its rapid and unique temporal variation of the Earth's field (Kotzé 2003; Mandea et al. 2007). Subsequently, a statistical analysis was undertaken to investigate and compare the model predictions of IGRF-12, CHAOS-6 and POMME-10 with 2015 Southern African D (declination), H (horizontal component), Z (vertical component) and F (total field) observatory and field survey measurements. Both main field (MF) and secular variation (SV) for D, H, Z and F will be evaluated.

## Data and method of evaluation

In Southern Africa, continuous recording of geomagnetic field is done at 4 INTERMAGNET (www.intermagnet.org) geomagnetic observatories located at Hermanus (HER) and Hartebeesthoek (HBK) in South Africa and at Tsumeb (TSU) and Keetmanshoop (KMH) in Namibia. Their locations are shown in Fig. 1 together with the current Southern African geomagnetic survey network consisting of 40 repeat stations with an average spatial separation of 301.4 km, varying between a minimum distance of 176.5 km and a maximum distance of 470.2 km between nearest stations. These repeat stations have been occupied since 2005 on an annual basis in order to characterise the secular variation in Southern Africa more accurately in comparison with the previous practice of 5-year intervals. A study by De Santis et al. (2013) also concluded that repeat station field surveys should be done more frequently than 5 years in order to improve secular variation models. The error estimates at the observatories for H and Z components vary from 1 nT at HER to 1.5 nT for a remote location such as TSU or KMH, depending on the accuracy of the baselines.

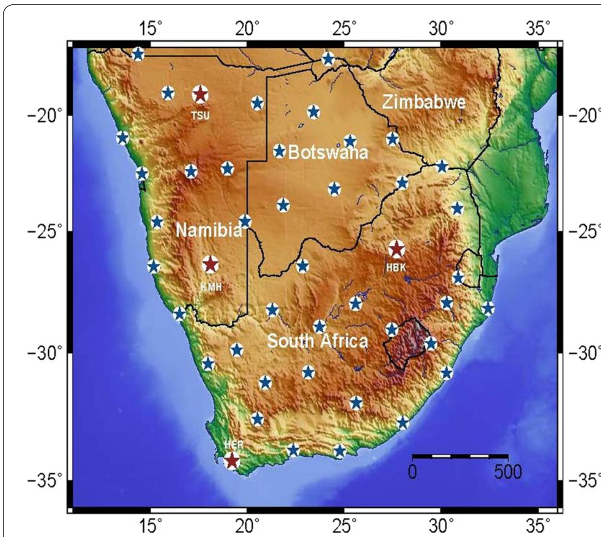


**Fig. 1** A map of Southern Africa showing the positions of the 4 INTERMAGNET observatories, HER, HBK, KMH and TSU (*red stars*), as well as the positions of the repeat stations (*blue stars*). A scale in km to provide an indication of the distances between the various locations is also included

Similarly for D, the errors can vary from 10″ at HER to 20″ at places like TSU and KMH where less frequent absolute observations are made.

All the repeat stations are marked by concrete beacons, ensuring that all observation points are exactly reoccupied during successive surveys (Newitt et al. 1996; Barraclough and De Santis 2011). Vector field observations at each station are as a rule done in the early evening around 20h00 (LT) and early morning around 04h00 (LT), with a three-component fluxgate variometer operating continuously and during the night. Corrections for diurnal and other short-term external field variations are subsequently made by reducing field station observations to nighttime average values (see Korte et al. 2007 for details). This methodology proved to be a great improvement to the exclusive use of magnetic observatories which are sometimes located away at a distance of several hundred km. An estimate of measurement uncertainties is obtained from the scatter of the individual results at a particular repeat station and any observed systematic difference between evening and morning observations. This provides error estimates of 1–2 nT in H and Z and 0.3–0.5 min in D which can to a large extend be attributed to a combination of observation and azimuth position uncertainties.

Two data sets comprising of observatory and repeat station annual main field and secular variation information were used in this investigation:

*Main field data* The repeat station measurements were taken between middle of September and middle of December during 2015. As secular variation is negligibly small compared to the strength of the main field, all repeat station nighttime results are taken as representative of the 2015 main field. This repeat station data set was augmented by standard observatory annual means, averaged over all hours of a year and centred on the middle of 2015.

*Secular variation data* Annual secular variation values for the repeat stations were obtained as first differences between 2014 and 2015 main field data divided by the time interval in years. As individual stations in general were visited at about the same time of the month for both years, the first differences eliminated not only crustal biases but also large parts of annual external field variations. Annual secular variation at the observatories was also obtained by first differences of standard annual mean values. In the process, 120 vector differences from 40 repeat stations and 12 vector differences from the 4 observatories could be obtained for 2015.

It was also necessary for this study to remove any crustal anomalies from all observatories as well as repeat station beacons locations. For this purpose, the crustal anomaly field model MF7 (http://geomag.org/models/MF7.html) with maximum degree 133 was subtracted from all 2015 main field data. The field survey data values were further corrected for ionospheric (plus induced) fields as well as large-scale magnetospheric (plus induced) fields using the CM4 comprehensive field model (Sabaka et al. 2004) by calculating average external field estimates for the time interval during which measurements at each repeat station were taken. For the observatory main field components however, average mean external field contributions were determined by calculating 8760 hourly values for D, H, Z and F, respectively. This procedure enabled us to compare predominantly only core field measurements with model predictions.

## Results and discussion

Results of the statistical comparisons between measured and modelled main field and secular variation components are summarised in Table 1.

Root-mean-square (RMS) differences (observations model) are shown in Fig. 2. From Table 1a, it is clear that all models underestimate the D, while all models overestimate H, Z and F. An equality of mean test (Student's *t*) as well as variance test (*F*-test) revealed that these differences are indeed statistically significant (Joanes and Gill 1998). On average, all 3 models used in this study describe main field D and H, Z and F equally well. Although the absolute RMS value for H is 2.4 times smaller than the RMS for Z and 2.1 times smaller than the RMS for F, it does not mean that H is better represented than Z or F. These ratios are actually reflections of the fact that the individual components have almost the same relative errors in comparison with their respective values in Southern Africa. In the case of secular variation however, it has been found that the relative error in H is much larger than the relative errors in Z and F for all 3 models. A possible explanation for this is an abrupt change in the secular variation patterns of both the X and Y components during 2014–2015. Typical examples of the misfit of the models to the Southern African geomagnetic field data for D, H, Z and F can be seen in Figs. 3, 4, 5 and 6, respectively. Residual values for D vary between −80 and 80 min, while the average misfit is approximately 9 min. for all three models. With a skewness value of −0.3 min, one can safely assume that the misfit follows a normal distribution. In the case of H, the model misfit ranges between −200 and 120 nT, with a mean of approximately −15 nT. This small overestimation of H by all three models, together with a skewness factor of −0.3, indicates that this misfit distribution is a normal distribution for all practical purposes. From Table 1a, the CHAOS-6 model provides the smallest average deviation

**Table 1 Statistics for the differences between geomagnetic field measurements and IGRF-12, CHAOS-6 and POMME-10 models over Southern Africa regarding main field (a) and secular variation (b) for D, H, Z and F components**

| Model/component | IGRF-12 | CHAOS-6 | POMME-10 |
|---|---|---|---|
| (a) Main field | | | |
| D | | | |
| RMS (min) | 33.2 | 32.9 | 33.2 |
| Mean (min) | 9.2 | 9.1 | 9.5 |
| $\sigma$ (min) | 32.3 | 32.1 | 32.2 |
| Skewness | −0.28 | −0.3 | −0.29 |
| Student's *t* | 0.077 | 0.08 | 0.069 |
| *F*-test | 0.93 | 0.95 | 0.94 |
| H | | | |
| RMS (nT) | 73.2 | 73.2 | 73.6 |
| Mean (nT) | −16.6 | −13.3 | −14.5 |
| $\sigma$ (nT) | 72.2 | 72.9 | 72.8 |
| Skewness | −0.25 | −0.23 | −0.23 |
| Student's *t* | 0.15 | 0.25 | 0.21 |
| *F*-test | 0.99 | 0.99 | 0.99 |
| Z | | | |
| RMS (nT) | 178.9 | 178.5 | 178.6 |
| Mean (nT) | −26.7 | −17.9 | −25.5 |
| $\sigma$ (nT) | 179.2 | 179.8 | 178.9 |
| Skewness | 0.3 | 0.3 | 0.35 |
| Student's *t* | 0.35 | 0.53 | 0.37 |
| *F*-test | 0.88 | 0.87 | 0.88 |
| F | | | |
| RMS (nT) | 157.1 | 157.3 | 156.9 |
| Mean (nT) | −17.3 | −10.8 | −17.1 |
| $\sigma$ (nT) | 158.2 | 159.0 | 158.1 |
| Skewness | −0.64 | −0.63 | −0.70 |
| Student's *t* | 0.50 | 0.67 | 0.51 |
| *F*-test | 0.96 | 0.95 | 0.96 |
| (b) Secular variation | | | |
| D | | | |
| RMS (min/year) | 1.6 | 1.17 | 1.35 |
| Mean (min/year) | 1.13 | 0.46 | 0.82 |
| $\sigma$ (min/year) | 1.15 | 1.09 | 1.08 |
| Skewness | −1.56 | −2.44 | −2.02 |
| Student's *t* | 2.5E−07 | 1.1E−02 | 2.2E−05 |
| *F*-test | 0.61 | 0.84 | 0.95 |
| H | | | |
| RMS (nT/year) | 6.3 | 5.5 | 8.8 |
| Mean (nT/year) | 2.0 | 1.78 | 7.08 |
| $\sigma$ (nT/year) | 6.1 | 5.27 | 5.32 |
| Skewness | −0.17 | −0.64 | −0.7 |
| Student's *t* | 4.3E−02 | 3.9E−02 | 2.6E−10 |
| *F*-test | 0.44 | 0.84 | 0.94 |
| Z | | | |
| RMS (nT/year) | 6.6 | 3.6 | 6.9 |
| Mean (nT/year) | −4.7 | −0.95 | 6.32 |
| $\sigma$ (nT/year) | 4.7 | 3.53 | 2.92 |
| Skewness | 0.16 | 0.14 | 0.15 |
| Student's *t* | 1.9E−07 | 9.6E−02 | 1.7E−16 |
| *F*-test | 0.10 | 0.69 | 0.98 |
| F | | | |
| RMS (nT/year) | 11.7 | 11.8 | 9.2 |
| Mean (nT/year) | 5.5 | −3.3 | −1.9 |
| $\sigma$ (nT/year) | 10.4 | 11.8 | 9.1 |
| Skewness | −0.99 | −0.5 | −1.5 |
| Student's *t* | 2.2E−03 | 0.39 | 0.19 |
| *F*-test | 2.9E−02 | 0.43 | 0.42 |

Standard deviation values are presented by $\sigma$

for all components over Southern Africa although the RMS value for all 3 main field models is the same for all practical purposes. A typical example of the Z misfit with respect to the geomagnetic field observations can be seen in Fig. 5. Figure 5 also shows that, except for one or two isolated positions, e.g. Mica (−24.17°, 30.83°) in South Africa and Francistown (−21.6°, 27.5°) in Botswana where the misfits can be regarded as outliers, the average misfit varies between ±200 nT. A skewness parameter of 0.3 ensures a nearly normal distribution of model misfit to field observations.

RMS differences between secular variation observations and model estimates can be seen in Fig. 2b and Table 1b. This shows that the CHAOS-6 model provides the best secular variation estimate for D, H and Z over Southern Africa from an RMS point of view. For F however, the POMME-10 model provides the best fit to observations. An equality of mean test (Student's *t*) as well as variance test (*F*-test) revealed that these differences are indeed statistically significant. It is significant to notice that a similar comparative evaluation of IGRF candidate secular variation models for 1995 (Kotzé 1997) showed that the CHAOS-6 secular variation model provided significantly better fits to 2015 observations for D, H and Z. This finding provides further evidence of the importance of high accurate satellite and observatory data, particularly for an area such as Southern Africa with its rapid and unpredictable secular variation character. The largest negative skewness factors were obtained for D for all 3 secular variation models, while in the case of both H and Z the skewness factors are close to zero, indicating near-symmetrical misfit distributions.

Typical examples of the misfit of the secular variation models to the Southern African geomagnetic data for D, H, Z and F can be seen in Figs. 7, 8, 9 and 10, respectively.

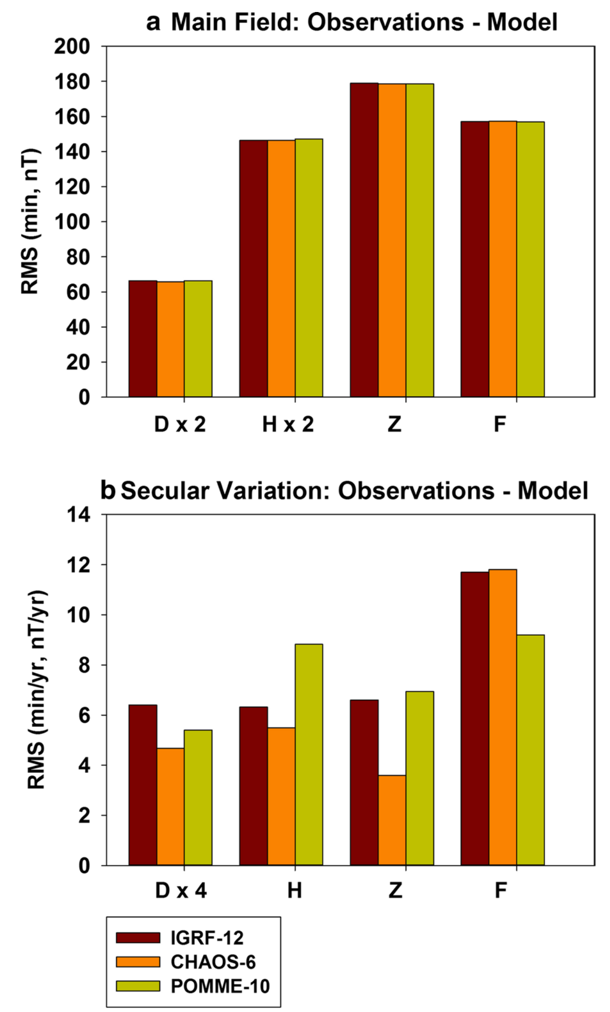


**Fig. 2** RMS differences between D, H, Z and F geomagnetic field components and IGRF-12, CHAOS-6, POMME-10 global field models over Southern Africa regarding main field (**a**) and secular variation (**b**). Results for the regional field model for Southern Africa, SAREG, are also shown for comparative purposes. Both the main field declination D and the horizontal component H were scaled up by a factor of 2 in order to match the scale of the bar chart, while the secular variation for D was scaled by 4

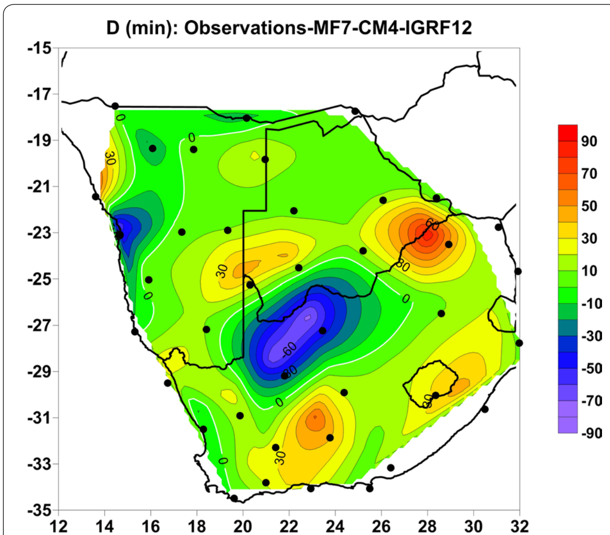


**Fig. 3** Contour plot of the misfit of IGRF-12 to Southern African declination (D) observations after subtracting crustal anomalies (MF7) and external field variations as determined by the CM4 model. The positions of the observation locations are indicated by *dots*, while the *zero contour line* is indicated in *white*

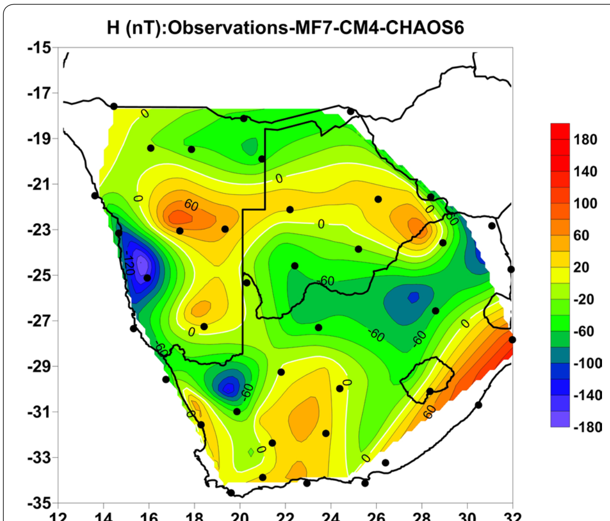


**Fig. 4** Misfit contour plot of CHAOS-6 to horizontal component observations of Southern Africa after correcting for crustal biases using the MF7 model and external field variations as given by the CM4 field model. The positions of the observation locations are indicated by *dots*, while the *zero contour line* is indicated in *white*

In addition, the positions of the observation locations are indicated by dots, while the zero contour line is marked in white.

Residual values for D secular variation misfit vary between −1.4 and 3.0 min/year, while the average misfit in the case of CHAOS-6 is approximately 0.5 min/year. With an average deviation between observation and model of 0.8 min/year, one can safely conclude that all 3 models underestimate the declination secular variation across Southern Africa. In the case of H secular variation, the model misfit ranges between −5 and 13 nT/year, with a mean of approximately 2.0 nT/year for both IGRF-12 and CHAOS-6, while in the case of POMME-10, the mean misfit is approximately 7 nT/year. One also notices that across the central part of Southern Africa, all the models overestimate H secular variations, while in the north-western as well as the south-eastern part of the region, the models tend to underestimate observations (Fig. 8). The Z secular variation misfit between

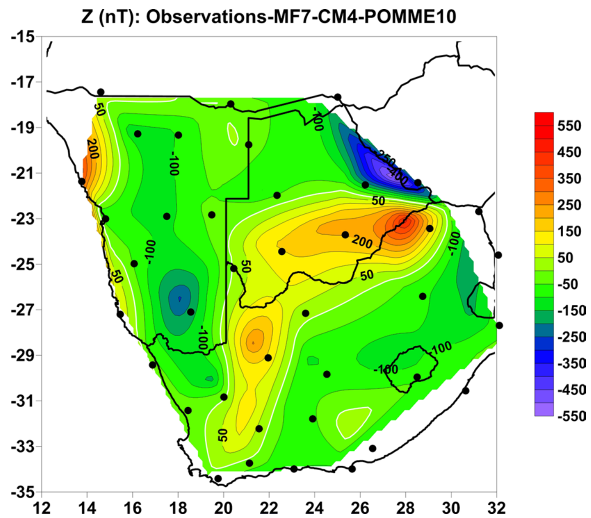


**Fig. 5** Misfit contour plot for Z observations of Southern Africa by the POMME 10 model after corrections for crustal field bias using MF7, and external magnetospheric and ionospheric perturbations as determined by CM4 have been applied. The positions of the observation locations are indicated by *dots*, while the *zero contour line* is indicated in *white*

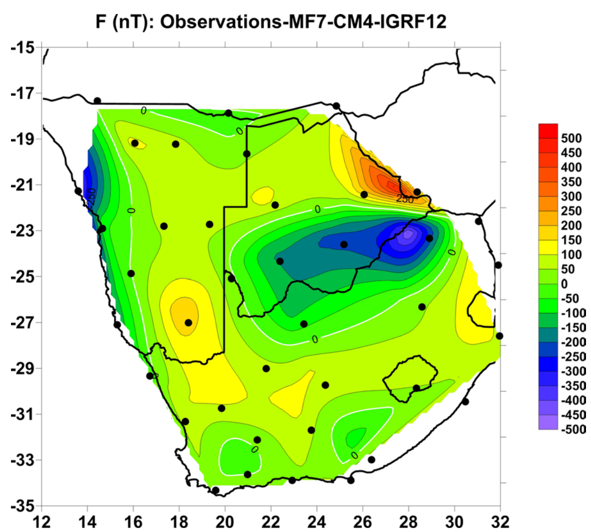


**Fig. 6** Misfit contour plot for F observations of Southern Africa by the IGRF 12 model after corrections for crustal field bias using MF7, and external magnetospheric and ionospheric perturbations as determined by CM4 have been applied. The positions of the observation locations are indicated by *dots*, while the *zero contour line* is indicated in *white*

2015 observations and model predictions in the case of IGRF-12, shown in Fig. 9, indicates that the misfit varies between an overestimation in the north-western part of Namibia and an underestimation in the south-eastern part of South Africa. Similar patterns have been obtained

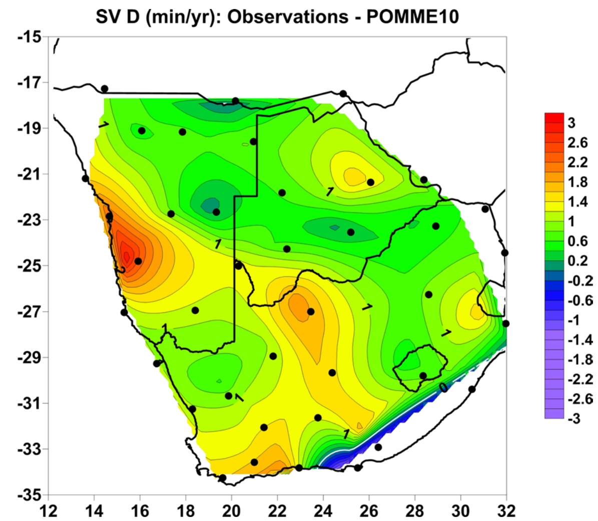


**Fig. 7** Contour plot showing the misfit between 2015 declination secular variation observations and POMME-10 model predictions

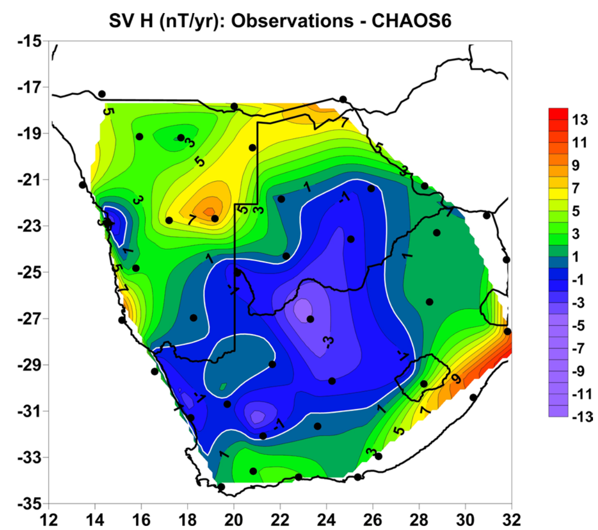


**Fig. 8** Contour plot of the misfit between H secular variation observations and CHAOS-6 for 2015

for POMME-10 and CHAOS-6. The latter secular variation model also provides the best approximation for 2015 observations as evidenced by an RMS value of 3.6 nT/year and a mean of −0.95 nT/year. With an average skewness factor of 0.14, one can safely assume that the misfit distributions for all 3 secular variation models are highly symmetrical. Total field F secular variation is underestimated by all 3 models with POMME-10 providing the best fit to observations. Figure 10 is a typical example of the misfit contour plot in the case of IGRF-12, showing that the largest underestimation is in the south-eastern part of Southern Africa, while the largest overestimation

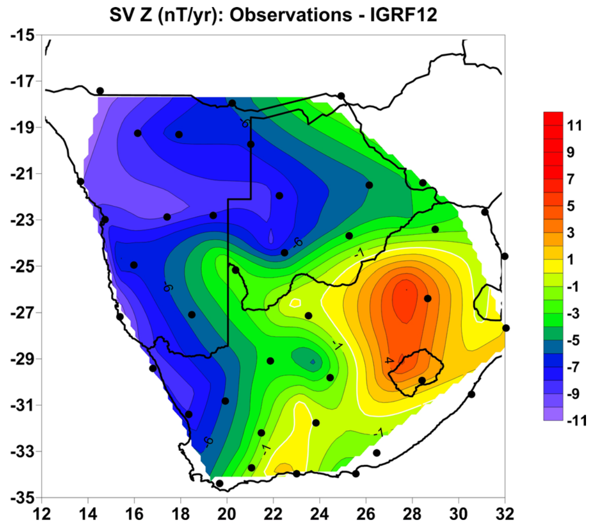


**Fig. 9** Contour plot between Z secular variation observations over Southern Africa and IGRF-12 model for 2015

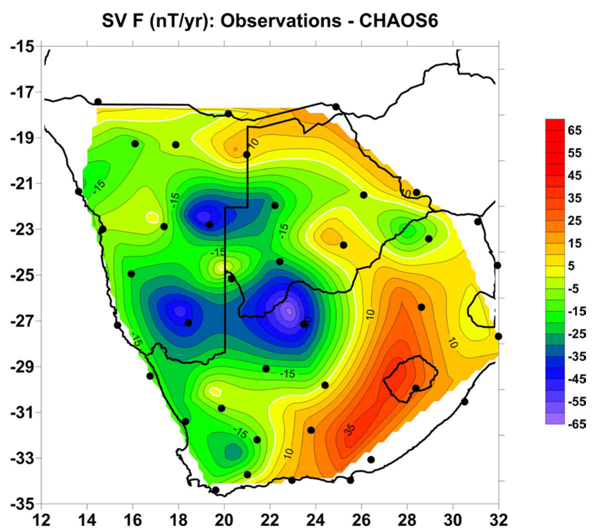


**Fig. 10** Contour plot of the misfit between F secular variation observations and IGRF-12 for 2015

takes place across the central part of Southern Africa. The Severn repeat station (−26.58°, 22.85°) can be regarded as an outlier in terms of both H and F secular variation.

## Conclusions

A feature of this comparative statistical evaluation of IGRF-12, CHAOS-6 and POMME-10 geomagnetic field models in terms of their agreement with repeat station field survey and observatory data over Southern Africa is their similarity in terms of main field D, H, Z and F components for 2015. No single model is significantly superior to the others, in spite of the fact that both IGRF-12 and POMME-10 do not include 2015 ground-based data for Southern Africa. On the other hand, CHAOS-6 is partly based on monthly mean data from 160 observatories till March 2016, including Hermanus, Hartebeesthoek, Tsumeb and Keetmanshoop in Southern Africa, a region characterised by rapid and irregular secular variation changes (Kotzé 2003, 2017). The inclusion of this data in the derivation of CHAOS-6 is evident in the fit of this model to ground-based secular variation data across Southern Africa for 2015, rendering it the most accurate of all 3 secular variation models used in this evaluation, except in the case of F where the POMME-10 model provides the best fit to the observations. One can also conclude that the use of quasi-definitive near-real-time observatory data is essential to capture sudden changes in secular variation patterns. The inclusion of high-quality satellite geomagnetic field data in the derivation of global field models should not be underestimated. A comparison with results obtained in a similar evaluation of 1995 secular variation candidate IGRF and DGRF models over Southern Africa reveals a substantial improvement in the fit of present-day global secular variation models. The inclusion of repeat station data in the derivation of global spherical harmonic secular variation models, even in a weighted ratio of 0.1:1 to observatory data, might be an interesting experiment that can provide new constraints particularly over regions characterised by rapid time-varying geomagnetic field components.

**Acknowledgements**

The CHAOS-6 field model coefficients used in this investigation were downloaded from the website http://www.spacecenter.dk/files/magneticmodels. The POMME 10 model coefficients were obtained at http://www.geomag.org/models/pomme10.html, while the MF7 model coefficients were downloaded from http://www.geomag.org/models/MF7.html. The IGRF-12 model coefficients on the other hand were obtained at http://www.ngdc.noaa.gov/IAGA/vmod/igrf/html. PK was supported by an NRF grant (no. 103610) for rated researchers. The support provided by the German Centre for Geosciences (GFZ) in Potsdam to run and maintain the Keetmanshoop magnetic observatory according to INTERMAGNET standards is appreciated. This work is based on research supported in part by the National Research Foundation of South Africa (Grant Number 103610).

**Competing interests**

The author declares that he has no competing interests.

## Publisher's Note

Springer Nature remains neutral with regard to jurisdictional claims in published maps and institutional affiliations.

Received: 2 March 2017 Accepted: 11 June 2017
Published online: 22 June 2017

**References**

Barraclough DR, De Santis A (2011) Repeat station activities. In: Korte M, Mandea M (eds) Geomagnetic observations and models. Springer, Berlin, pp 45–55

De Santis A, Qamili AE, Cianchini G (2013) Repeat station surveys: implications from chaos and ergodicity of the recent geomagnetic field. Ann Geophys 56:1–7
Finlay CC et al (2016) Recent geomagnetic secular variation from SWARM and ground observatories as estimated in the CHAOS-6 geomagnetic field model. Earth Planets Space 28:112. doi:10.1186/s40623-016-0486-1
Joanes DN, Gill CA (1998) Comparing measures of sample skewness and kurtosis. J R Soc (Ser D) Stat 47(1):183–189
Korte M, Mandea M, Kotzé PB, Nahayo E, Pretorius B (2007) Improved observations at the southern African geomagnetic repeat station network. S Afr J Geol 110:175–186. doi:10.2113/gssajg.110.2-3.175
Kotzé PB (1997) A comparative evaluation for the southern African region of DGRF90 and IGRF95 candidate models. J Geomag Geoelectr 49:347–352
Kotzé PB (2003) The time-varying geomagnetic field of Southern Africa. Earth Planets Space 55:111–116. doi:10.1186/BF03351738
Kotzé PB (2017) The 2014 geomagnetic jerk as observed by southern African magnetic observatories. Earth Planets Space 69:17. doi:10.1186/s40623-017-7
Langel RA, Estes RH (1985) The near-Earth magnetic field at 1980 as determined from MAGSAT. J Geophys Res 90:2495–2510
Mandea M, Korte M, Mozzoni D, Kotze P (2007) The magnetic field changing over the southern African continent—a unique behaviour. S Afr J Geol 110:193–202
Newitt L R, C E Barton, J Bitterly (1996) Guide for magnetic repeat station survey, IAGA, p 112, ISBN:0-9650686-1-7
Olsen N (2002) A model of the geomagnetic field and its secular variation for epoch 2000 estimated from Ørsted data. Geophys J Int 149:454–462
Olsen N, Friis-Christiansen E, Floberghagen R (2013) The *Swarm* Satellite Constellation Application and Research Facility (SCARF) and *Swarm* data products. Earth Planet Space 65:1. doi:10.5047/eps.2013.07.001
Sabaka TJ, Olsen N, Langel RA (2004) Extending comprehensive models of the Earth's magnetic field using Ørsted and CHAMP data. Geophys J Int 159:521–547
Thébault E, Finlay CC, Toh H (2015) Evaluation of candidate geomagnetic field models for IGRF-12. Earth Planets Space 67:112. doi:10.1186/s40623-015-0273-4